Disulphide production by Ero1alpha-PDI relay is rapid and effectively regulated

Appenzeller-Herzog, Christian and Riemer, Jan and Zito, Ester and Chin, King-Tung and Ron, David and Spiess, Martin and Ellgaard, Lars

Originally published as:

Appenzeller-Herzog, Christian and Riemer, Jan and Zito, Ester and Chin, King-Tung and Ron, David and Spiess, Martin and Ellgaard, Lars. (2010) Disulphide production by Ero1alpha-PDI relay is rapid and effectively regulated. The EMBO journal, Vol. 29, H. 19. S. 3318-3329.

Disulfide production by Ero1α–PDI relay is rapid and effectively regulated

Christian Appenzeller-Herzog[1,2,5,7], Jan Riemer[1,6], Ester Zito[3], King-Tung Chin[3], David Ron[3,4], Martin Spiess[2], Lars Ellgaard[1,7]

[1]Department of Biology, University of Copenhagen, 2200 Copenhagen N, Denmark

[2]Biozentrum, University of Basel, 4056 Basel, Switzerland

[3]Skirball Institute of Biomolecular Medicine, New York University School of Medicine, New York, NY 10016

[4]Institute of Metabolic Science, University of Cambridge, United Kingdom, CB2 0QQ

[5]Current address: Department of Pharmaceutical Sciences, University of Basel, 4056 Basel, Switzerland

[6]Current address: Department of Cell Biology, University of Kaiserslautern, 67663 Kaiserslautern, Germany

[7]Corresponding authors: Lars Ellgaard, email: lellgaard@bio.ku.dk, Tel: +45 35 32 17 25, Fax: +45 35 32 21 28. Christian Appenzeller-Herzog, email: christian.appenzeller@unibas.ch, Tel: +41 61 267 14 86, Fax: +41 61 267 15 15

Character count: 54,110

Running title: Ero1α- and PDI-mediated ER redox regulation

Subject Category: Proteins

Abstract

The molecular networks that control endoplasmic reticulum (ER) redox conditions in mammalian cells are incompletely understood. Here, we demonstrate that after reductive challenge the ER steady-state disulfide content is restored on a time scale of seconds. Both the oxidase Ero1α and the oxidoreductase protein disulfide isomerase (PDI) strongly contribute to the rapid recovery kinetics, but experiments in ERO1 deficient cells indicate the existence of parallel pathways for disulfide generation. We find PDI to be the main substrate of Ero1α, and mixed-disulfide complexes of Ero1 primarily form with PDI, to a lesser extent with the PDI-family members ERp57 and ERp72, but are not detectable with another homologue TMX3. We also demonstrate for the first time that the oxidation level of PDIs and glutathione is precisely regulated. Apparently this is achieved neither through ER import of thiols nor by transport of disulfides to the Golgi apparatus. Instead, our data suggest that a dynamic equilibrium between Ero1- and glutathione disulfide-mediated oxidation of PDIs constitutes a key element of ER redox homeostasis.

Key words: Disulfide-Bond Formation / Endoplasmic Reticulum / Ero1 / Glutathione / Protein Disulfide Isomerase

Introduction

Regulation of the redox environment in the endoplasmic reticulum (ER) is emerging as a key aspect of cellular homeostasis (Malhotra and Kaufman, 2007; Merksamer *et al*, 2008), and the thiol-disulfide oxidoreductases of the protein disulfide isomerase (PDI) family are central to ER redox control (Appenzeller-Herzog and Ellgaard, 2008b). PDIs contain one or more thioredoxin-like domains. These typically harbor a CXXC active-site sequence motif required for the catalysis of thiol-disulfide exchange reactions, such as the introduction of disulfides into substrate proteins.

The identification in yeast of the essential ER-resident sulfhydryl oxidase Ero1p (Frand and Kaiser, 1998; Pollard *et al*, 1998), which oxidizes PDI (Frand and Kaiser, 1999; Tu *et al*, 2000) and reduces molecular oxygen to hydrogen peroxide (Gross *et al*, 2006), has led to an improved understanding of oxidative folding and ER redox regulation (Sevier and Kaiser, 2008; Sevier *et al*, 2007). Consistent with a key function in ER protein oxidation, both human isoforms Ero1⟨ and Ero1® are transcriptionally upregulated by the ER stress response (Marciniak *et al*, 2004; Pagani *et al*, 2000), which can be associated with a reductive shift in the ER redox conditions (Merksamer *et al*, 2008; Nadanaka *et al*, 2007). Moreover, the activity of Ero1α is subject to negative feedback regulation by intramolecular disulfide bonds (Appenzeller-Herzog *et al*, 2008; Baker *et al*, 2008). The enzyme appears in at least three redox forms; reduced, OX1, and OX2 (Benham *et al*, 2000). The latter is the most oxidized form with all regulatory disulfide bonds in place ((Appenzeller-Herzog *et al*, 2008); our unpublished observations). The cellular activation state of Ero1α is controlled by the availability of reduced PDI (Appenzeller-Herzog *et al*, 2008), which can reduce the regulatory disulfide bonds (see also Discussion) (Appenzeller-Herzog

et al, 2008; Baker *et al*, 2008; Sevier *et al*, 2007). Ero1α also controls calcium fluxes from ER to mitochondria (Li *et al*, 2009), which could correlate with its partial localization at mitochondria-associated ER membrane domains (Gilady *et al*, 2010).

The dominance of Ero1 enzymes in providing the oxidizing equivalents for the synthesis of disulfides is, however, still a matter of debate (Thorpe and Kodali, 2010). For instance, the slow *in vitro* rate of PDI oxidation by Ero1〈 (Baker *et al*, 2008; Wang *et al*, 2008) appears at odds with a principal function in disulfide-bond generation. Knockout of the single Ero1 gene in fruit fly causes a specific defect in Notch signaling while apparently leaving the bulk disulfide-bond repertoire unperturbed (Tien *et al*, 2008). Most importantly, however, Ero1α and Ero1β appear non-essential in the mouse, as evidenced by the viability of an Ero1α/Ero1β double mutant (Zito *et al*, 2010). Indeed, several possible Ero1-independent pathways for disulfide generation and/or the oxidation of PDI in the ER of mammalian cells exist (Margittai and Banhegyi, 2010). These include the activity of quiescin-sulfhydryl oxidases (Thorpe and Kodali, 2010), import of dehydroascorbate from the cytosol and its reduction by dithiol groups (Saaranen *et al*, 2010), ER-luminal detoxification of NADPH oxidase 4-generated hydrogen peroxide (Santos *et al*, 2009), and a pathway that uses the oxidizing equivalents of radicals derived from mitochondrial respiration to generate disulfides in secretory compartments (Yang *et al*, 2007). In analogy to a mechanism that operates in both archaea and bacteria (Dutton *et al*, 2008; Singh *et al*, 2008), PDI could also be oxidized through the vitamin K cycle (Wajih *et al*, 2007). Currently, we lack a thorough cell biological understanding of these pathways in relation to oxidative folding in the ER.

In addition to the PDIs and Ero1, glutathione also plays a fundamental role in ER redox homeostasis. This low-molecular weight thiol compound exists as a mixture of reduced glutathione (GSH) and glutathione disulfide (GSSG). Cytosol-derived GSH can enter the ER where its reducing power is required for the rearrangement of aberrant disulfide bonds in folding substrates (Chakravarthi *et al*, 2006).

On these premises, we decided to further explore the links between Ero1, PDIs, and glutathione in cultured human cells. Our work demonstrates a very rapid production of disulfides in the ER whose velocity depends on both Ero1〈 and PDI, but apparently less so on other PDI family members. In cells devoid of both Ero1α and β, however, we present evidence for Ero1-independent pathway(s) for thiol oxidation. Finally, we show that ER oxidation is tightly regulated, and propose a mechanistic model of ER redox homeostasis that integrates previous and current findings.

Results

Thiol import and disulfide export play a minor role in acute ER redox control

While it has been shown that Ero1 activity ultimately leads to the oxidation of GSH in the ER (Appenzeller-Herzog *et al*, 2008; Cuozzo and Kaiser, 1999), the mechanisms that counteract the accumulation of ER-luminal GSSG are still unclear (Chakravarthi *et al*, 2006; Thorpe and Kodali, 2010). Since GSSG displays only low permeability through microsomal membranes (Banhegyi *et al*, 1999), we tested whether export of GSSG through the secretory pathway might contribute to ER redox homeostasis. We therefore combined the pharmacological inhibition of ER-to-Golgi transport with ER redox state analysis. For this purpose, we used a combination of brefeldin A and monensin (BFA/mon), which blocks vesicular anterograde transport from the ER while preserving the integrity of the Golgi apparatus ((Barzilay *et al*, 2005); Fig. S1), and an assay in which oxidized active-site cysteines in PDIs are modified with 4-acetamido-4´-maleimidylstilbene-2,2´-disulfonic acid (AMS) resulting in slower mobility upon SDS-PAGE (Jessop and Bulleid, 2004). Using this AMS shift assay, we have consistently found the redox distribution of various PDIs to exhibit molecules in both reduced and oxidized states (Appenzeller-Herzog and Ellgaard, 2008a; Appenzeller-Herzog *et al*, 2008; Haugstetter *et al*, 2005; Roth *et al*, 2010), the ratio of which can be used as a readout to monitor redox variations in the ER.

We studied the effect of BFA/mon treatment on the redox recovery of the PDIs TMX3 (a transmembrane PDI family member) and ERp57 (a close homolog of PDI) upon application and washout of the oxidant diamide. No significant delay in the recovery was observed under conditions of blocked ER-to-Golgi transport (Figs. 1A

and B). Hence, BFA/mon-sensitive vesicular export appears to be of minor importance as a redox-balancing mechanism against hyper-oxidizing conditions.

Reestablishment of the ER redox state after washout of the oxidant dipyridyl sulfide is mediated by the import of GSH through the ER membrane (Jessop and Bulleid, 2004). Further reductive input is brought to the ER through the co-translational translocation of protein thiols (Cuozzo and Kaiser, 1999). For these reasons, we examined if lowering cellular GSH levels by L-buthionine-sulfoximine (BSO) or the shutdown of translation by cycloheximide (CHX) altered the steady-state ER redox state. As shown in Fig. 1C, neither of these drugs showed a consistent effect on the redox ratios of TMX3 and ERp57 at steady state. It should be noted that for reasons of cytotoxicity we did not apply combinations of the above treatments so that additive effects between the different reductive pathways cannot be excluded. Still, these results suggested that mechanism(s) other than ER export of disulfides or import of thiols secure ER redox balance.

PDI withstands in situ reduction better than other ER oxidoreductases

PDI is a known substrate of Ero1 (Sevier and Kaiser, 2008). It is, however, less clear what regulates the redox state of other ER oxidoreductases and whether they are substrates of Ero1 (Jessop *et al*, 2009; Kulp *et al*, 2006; Mezghrani *et al*, 2001). We therefore next investigated factors that could control the redox state of various PDI family members. First, we determined their *in vivo* dithiothreitol (DTT) resistance by means of an assay where cells are challenged with increasing concentrations of this membrane-permeant reductant. Although the two separate active-site domains in PDI exhibit very similar reduction potentials (Darby and Creighton, 1995), the

susceptibility towards DTT-mediated *in situ* reduction of the **a** domain was greater than of the **a´** domain (Fig. 2A). The **a´** domain is preferentially oxidized *in vitro* by Ero1α (Baker *et al*, 2008; Wang *et al*, 2008), which becomes activated by DTT through reduction of its regulatory disulfides (see below). Thus – although the DTT resistance readout could also be influenced by protein quaternary structure and differential accessibility of active-site cysteines to DTT or N-ethylmaleimide (NEM) – this result suggested that the DTT resistance of a PDI family member's active site in the ER reflects its propensity to become reoxidized by ER-resident oxidases.

When comparing the *in vivo* redox states of TMX3 and ERp57 after treatment of cells with different concentrations of DTT, we observed a slightly higher DTT resistance of the AMS-shifted form of ERp57 (Figs. 2B and C). This form represents ERp57 with its **a´** domain oxidized, while ERp57 with exclusively the **a** domain oxidized virtually co-migrates with the reduced form (Appenzeller-Herzog *et al*, 2008). Given that the active-site domains of ERp57 and TMX3 have approximately the same reduction potential (Frickel *et al*, 2004; Haugstetter *et al*, 2005), these results indicated that in cells the relative rates of oxidation for the single active site in TMX3 and the **a´** active site in ERp57 are distinct. Still, the Ero1α-controlled active site in PDI**a´** by far displayed the highest cellular DTT resistance, likely underlining its importance as an electron donor for Ero1α *in vivo*.

Mixed-disulfide interactions of PDIs with Ero1α and Ero1β reflect their in vivo DTT resistance

To investigate a possible role of Ero1 in maintaining the levels of the oxidized fractions of ERp57 and TMX3, we searched for intracellular mixed-disulfide

interactions. For this purpose, we performed co-immunoprecipitation experiments of myc-tagged Ero1α (Ero1αmyc6his) or Ero1β (Ero1βmyc6his) stably expressed from a doxycyclin-inducible promoter (Appenzeller-Herzog *et al*, 2008) using an *in situ* acidification/*in vitro* NEM-alkylation protocol. Compared to *in situ* NEM trapping, the acidification method was much more effective in trapping mixed-disulfide interactors of Ero1 (data not shown).

As expected, PDI was readily precipitated with αmyc in an Ero1αmyc6his-dependent fashion (Fig. 3A, lanes 3 and 4), and non-reducing gel electrophoresis revealed a prominent Ero1αmyc6his–PDI mixed-disulfide complex (Fig. 3A, lane 7). Unlike in a previous study that used NEM trapping of mixed disulfides (Mezghrani *et al*, 2001), an interaction with Ero1αmyc6his was also detected for ERp57 and ERp72 (Figs. 3B and C). While the pool of PDI acid-trapped in a covalent complex with Ero1αmyc6his at steady state was > 3% of total, the disulfide-linked fractions of ERp57 and ERp72 were only 0.5-2% (compare lane 4 to 1% of total in lane 1). In contrast, we detected no co-immunoprecipitation of TMX3 (Fig. 3D). The same pattern of mixed-disulfide interactions was also found for Ero1βmyc6his (Fig. 3, lanes 5 and 8). In the case of ERp57, HA-tagged mutants with one active site changed to SXXS could both be acid-trapped in a mixed-disulfide complex with Ero1αmyc6his or Ero1βmyc6his (Fig. S2A). Since the cells were pulsed with ^{35}S-methionine for 1 h in the presence of doxycyclin and chased for 1 h without doxycyclin but in the presence of CHX, the detected mixed disulfide is unlikely to involve a folding intermediate of Ero1. The same result was obtained in the absence of CHX (data not shown). Autoradiography of the membranes used for Western blotting documented the specificity of immunoprecipitation (Fig. S2B). Taken

together, Ero1α and β can form mixed disulfides not only with their known substrate PDI, but to a lesser extent also with ERp57 and ERp72, while TMX3 appears not to interact directly with either of the two oxidases.

Restoration of the ER redox balance is fast, precise, and affected by Ero1 over-expression

We next sought to functionally dissect the roles of Ero1 and its interaction partners in ER oxidation by means of an oxidative recovery assay. In this assay, the cellular levels of GSSG (which mainly represent GSSG in the ER (Appenzeller-Herzog *et al*, 2008)) are recorded at different time points after DTT washout. The oxidative resetting of the steady-state ratio of GSSG to total glutathione (GS_{tot}) in HEK293 cells was very precise and displayed a half time of only ~10 s (Figs. 4A and S3A). Similar recovery times were observed with a negative control cell line for doxycyclin-inducible over-expression of various Ero1 constructs (Fig. S3B). In this cell line, the reacquisition of the steady-state redox ratio of TMX3 and ERp57 was also very fast, with reoxidation becoming visible as early as 5 s after washout of the reductant (Fig. 4B and data not shown).

To study the effect of over-expression of exogenous Ero1 variants on the recovery of GSSG pools following a reductive challenge, we next performed DTT washout experiments in the Ero1αmyc6his- and Ero1βmyc6his-inducible cells. As expected, when doxycyclin was omitted, the rate of GSSG formation resembled the situation in non-transfected cells (Figs. 4C and D, control; for raw data see Fig. S3). In contrast, induction of Ero1αmyc6his strongly modulated the process. The initial rate of GSH oxidation was apparently too fast to be assessed by our experimental

setup so that around six times the steady-state GSSG levels were measured at the 0 s time point (Fig. 4C). However, consistent with our previous finding that over-expression of Ero1αmyc6his does not affect the cellular glutathione redox state (Appenzeller-Herzog *et al*, 2008), the GSSG:GS_{tot} ratio declined within 5 minutes to the steady-state value, indicating the reduction of excess GSSG to GSH.

In the case of Ero1βmyc6his over-expression, the peak in GSSG formation was clearly less prominent and did not occur until the 10 s time point (Fig. 4D). These differences were not a result of lower expression levels of Ero1βmyc6his ((Appenzeller-Herzog *et al*, 2008); Fig. S2B), and neither were they evident when monitoring the redox states of TMX3 and ERp57 upon DTT washout (Fig. S3C). We also used cell lines inducibly expressing two point mutants of Ero1α, Ero1αmyc6his-C131A and Ero1αmyc6his-C394A. While the former cannot build a critical regulatory disulfide, the latter is a competitive inhibitor of ER oxidation (Appenzeller-Herzog *et al*, 2008). Like Ero1αmyc6his, Ero1αmyc6his-C131A led to strong transient GSH hyper-oxidation (Fig. 4E). Conversely, expression of Ero1αmyc6his-C394A slightly impeded the rate of oxidative recovery (Fig. 4F).

Rapid oxidative recovery depends on Ero1 and PDI

The stimulation of ER reoxidation by exogenous Ero1 implies that endogenous Ero1 may catalyze the fast rate of disulfide-bond reformation upon DTT washout in non-transfected cells. To examine this, we first downregulated the expression of Ero1α in HEK293 cells by siRNA transfection. Partial knockdown of Ero1α slightly delayed ER reoxidation as assessed by timed redox analysis of TMX3 and ERp57 (Figs. S4A-

C). Next, we performed DTT washout experiments in embryonic fibroblasts derived from homozygous double mutant mice that harbor disruptive viral insertions in the genes encoding Ero1α and Ero1β (Zito *et al*, 2010). In keeping with the lack of Ero1α detection in double mutant cells (Fig. 5A), we observed a strong delay in ER reoxidation (Figs. 5B and C). The steady-state redox distribution of ERp57, however, was not affected by Ero1 deficiency (Fig. 5B). Unfortunately, these cells were not amenable to redox analysis of TMX3, because AMS modification only minimally shifts the electrophoretic mobility of mouse TMX3 (data not shown). We also assessed the reformation of GSSG during oxidative recovery from DTT in wild-type versus double mutant fibroblasts. Unexpectedly, the GSSG:GS_{tot} ratio promptly increased upon DTT washout not only in wild-type but also in the mutant cells, while complete reoxidation of GSH after a recovery period of 300 s was only achieved in wild-type cells (Fig. 5D). Furthermore, the resting value for GSSG:GS_{tot} was higher – i.e. more oxidizing – in double mutant cells (Fig. 5D, inset). These findings argue that at least one Ero1-independent pathway for GSH oxidation is operative in these cells.

We next investigated whether the efficient delivery of disulfide bonds in the ER depended on PDI. Indeed, for TMX3, ERp57, and glutathione, the oxidative recovery was clearly impaired in cells stably depleted of PDI (knockdown efficiency ~90%; see (Appenzeller-Herzog *et al*, 2008; Ou and Silver, 2006)) as compared to control cells (Figs. 5E-G). Thus, PDI plays a prominent role in oxidative recovery and the direct interactions of ERp57 or ERp72 with Ero1α (Fig. 3) cannot efficiently substitute the supply of disulfide bonds via the Ero1α–PDI relay. Nonetheless, the diminished rate of GSSG:GS_{tot} recovery in murine ERp57-/- cells (Garbi *et al*, 2006) suggested that early after DTT washout ERp57 does contribute to the shuttling of disulfide bonds to GSH (Fig. 5H).

So far, the data indicated that upon reductive challenge the propagation of Ero1-generated oxidative equivalents via PDI to the ER thiol pool was a rapid process. We therefore expected the complex between the two enzymes to form quickly after DTT treatment. To investigate this, we performed co-immunoprecipitation experiments using cells that had been challenged with DTT. Hence, doxycyclin-induced Ero1αmyc6his or Ero1βmyc6his cells were treated with DTT or left untreated, washed with ice-cold phosphate buffered saline (PBS) and covered with trichloroacetic acid (TCA) followed by αmyc immunoprecipitation. Co-immunoprecipitated PDI was readily detectable even after DTT treatment (Fig. 6A, lanes 12, 14, 16, 18), indicating the formation of the Ero1–PDI mixed-disulfide complexes to be extremely rapid. We suggest that this rapid process reflects the sulfhydryl oxidase activity of Ero1, and that this in turn accounts for the high apparent DTT resistance of the PDI**a´** active site (Fig. 2A). Notably, when analyzed under non-reducing conditions, the Ero1–PDI complexes isolated from DTT-treated cells migrated more slowly in the gel than when isolated from non-treated cells (Fig. 6A, Ero1+PDI RED.), a finding that was recapitulated for the endogenous proteins (Fig. 6B). This suggested that in untreated cells, the bulk of Ero1 that is covalently attached to PDI is in an oxidized or partially oxidized state. We also found the mixed-disulfide complex between PDI and Ero1α from DTT-treated cells to require the active-site Cys^{94} in Ero1α (Fig. 6C). Finally, covalent interactions of ERp57 with Ero1αmyc6his, Ero1βmyc6his, and endogenous Ero1α were not unequivocally detectable after DTT treatment (Fig. S5). Overall, the findings demonstrated that Ero1, when activated by DTT *in situ*, efficiently established a catalytic interaction with PDI.

Discussion

A molecular model for ER redox balance: interplay between Ero1 and glutathione

Although Ero1p is essential in yeast, the principal pathway for disulfide-bond generation in the ER of metazoans is still unclear (Thorpe and Kodali, 2010; Tien *et al*, 2008; Zito *et al*, 2010). Furthermore, the concept of disulfide delivery to reduced substrate proteins and GSH through Ero1–PDI relay has been questioned because it potentially leads to the futile depletion of cellular reductants accompanied by the accumulation of ER-luminal GSSG and hydrogen peroxide (Thorpe and Kodali, 2010).

The data presented herein provide new insight on the significance and the precise regulation of disulfide generation by Ero1. We show that reoxidation of PDI family members and GSH after reductive challenge is very fast. The recovery process is hampered by genetic ablation of Ero1 and by knockdown of PDI, indicating that the Ero1–PDI disulfide relay represents an important pathway for the production of disulfide bonds in the ER of mammalian cells. In most cell types including mouse embryonic fibroblasts (Dias-Gunasekara *et al*, 2005; Zito *et al*, 2010), this pathway is exclusively supported by the Ero1α isoform. In addition, the results demonstrate that – in spite of the oxidative burst in the ER following DTT treatment – accumulation of GSSG is very tightly regulated. Thus, the cellular GSSG:GS_{tot} ratio levels off to the steady-state value within a few minutes. This rapid process could neither be explained through import of GSH or nascent proteins from the cytosol, nor by the escape of disulfide-bonded molecules from the ER through the secretory pathway (Fig. 1).

Likewise, the diffusion of excess GSSG through the ER membrane is far too slow to efficiently counteract the luminal oxidation of GSH (Banhegyi *et al*, 1999). Instead, we propose that the prompt regulation of GSSG levels involves ER-luminal reduction of GSSG to GSH (see below).

The remarkable precision of GSSG:GS_{tot} regulation demonstrates a stringent redox control system in the ER. Here, PDI fulfills a central role in regulating ER redox conditions by its ability to adjust the activation state of Ero1α (Appenzeller-Herzog *et al*, 2008). Moreover, glutathione is known to be important for ER redox homeostasis, since its depletion compromises oxidative protein folding (Chakravarthi and Bulleid, 2004; Molteni *et al*, 2004) and sensitises the ER to over-expression of Ero1 (Appenzeller-Herzog *et al*, 2008). A model depicting central elements of ER redox regulation that integrates the PDI–Ero1α feedback loop with the redox buffering capacity of glutathione is presented in Fig. 7. We propose that a dynamic equilibrium exists between Ero1α-driven (Fig. 7A) and GSSG-driven (Fig. 7B) oxidation of substrate proteins via PDI family members. In the context of *de novo* disulfide formation driven by Ero1α, GSH is oxidized to GSSG. Rising levels of GSSG will promote GSSG-driven oxidation of PDIs and also shutdown of Ero1α. The interplay between the two oxidative pathways that either produce (Fig. 7A) or consume (Fig. 7B) ER-luminal GSSG maintains ER redox homeostasis by establishing a system that can adapt to physiological changes in the throughput of substrate proteins. It should be noted that this model does not exclude the contribution from Ero1-independent oxidative pathways (see also below). However, the exact influence on ER redox control of such pathways awaits further investigation.

The model is supported by our experiments using over-expression of Ero1 variants. The transient overshoot in GSH oxidation upon DTT washout resulting from the induction of Ero1αmyc6his (Fig. 4C) serves to illustrate both of the pathways depicted in Fig. 7. Hence, upon DTT-mediated breaking of the regulatory disulfides in Ero1α, the enzyme is present in its activated form which – when over-expressed – will catalyze excess production of GSSG via PDI. This process is, however, rapidly reverted. As indicated by the slightly delayed drop of $GSSG:GS_{tot}$ in Ero1αmyc6his–C131A expressing cells compared to wild-type (Figs. 4C and E), oxidative shutdown of Ero1α by the Cys^{94}–Cys^{131} regulatory disulfide (Appenzeller-Herzog *et al*, 2008; Baker *et al*, 2008) apparently modulates the process. A comparable delay in GSSG peak formation following DTT washout was observed upon over-expression of Ero1βmyc6his (Fig. 4D), which – like Ero1αmyc6his–C131A – is partially deregulated (Appenzeller-Herzog *et al*, 2008). Since GSSG levels still declined in both Ero1αmyc6his–C131A and Ero1βmyc6his cells, these experiments also point to the existence of additional regulatory disulfide bonds in Ero1α and Ero1β, e.g. the equivalent of Cys^{90}–Cys^{349} in Ero1p (Sevier *et al*, 2007). These in turn appear to be more stable in Ero1β, as evidenced by the less prominent formation of GSSG in Ero1βmyc6his cells upon DTT washout.

The decline of $GSSG:GS_{tot}$ in Ero1-over-expressing cells, however, cannot solely be explained by the shutdown of Ero1 activity, but must also involve reduction of GSSG. Based on *in vitro* kinetics, it has been proposed that GSSG in the ER preferentially reacts with reduced PDIs as compared to folding substrate proteins (Hatahet and Ruddock, 2009). Still, TMX3 and ERp57 – as putative electron sources for GSSG – were never completely oxidized during oxidative recovery in both

Ero1αmyc6his- and Ero1βmyc6his-expressing cells (Fig. S3C). A potential explanation for this observation could be that the PDIs rapidly pass on GSSG-derived disulfides to substrate proteins.

We suggest that GSSG-driven oxidation of PDIs also takes place in non-transfected cells to control redox homeostasis (Fig. 7B). For instance, TMX3, which is readily oxidized by GSSG *in vitro* (Haugstetter *et al*, 2007) but not found in mixed-disulfide complexes with Ero1 (Fig. 3D), showed rapid, Ero1α-dependent reoxidation upon DTT washout (Fig. S4B) presumably as a result of oxidation by GSSG. Altogether, we propose that the reaction of GSSG with reduced PDIs followed by substrate oxidation (Lyles and Gilbert, 1991; Zapun *et al*, 1998), a pathway that has received little attention since the discovery of Ero1, is of physiological relevance for oxidative protein folding and ER redox homeostasis.

The in vivo rate of Ero1-mediated disulfide generation is unexpectedly fast

The rapid kinetics of redox recovery after DTT washout observed here was unexpected since previously published data from mammalian (Enyedi *et al*; Mezghrani *et al*, 2001) and yeast cells (Cuozzo and Kaiser, 1999) reported the rate of Ero1-dependent ER reoxidation to be much slower. How can this be explained? In our experiments, we observed that the millimolar concentrations of DTT necessary to fully reduce GSSG and ER oxidoreductases *in situ* are difficult to wash away. Therefore, the slow recovery kinetics previously observed could in part have been due to residual DTT in the sample. In addition, the oxidation state of cellular glutathione in yeast at “time point zero” after DTT washout was not – as should be expected after DTT treatment – fully reduced ((Cuozzo and Kaiser, 1999; Sevier *et al*, 2007); P.

Nørgaard and J.R. Winther, personal communication). This suggests that considerable amounts of GSSG had already formed in the ER before quenching. The subsequent slow increase of GSSG could potentially reflect the vacuolar accumulation of ER-derived GSSG.

When assessed *in vitro*, the reaction kinetics of thiol-disulfide exchange between Ero1α and PDI are surprisingly slow compared to the rapid reaction in the ER during DTT washout (Baker *et al*, 2008; Wang *et al*, 2008). A partial explanation is offered by the shut-down of Ero1α activity through formation of intramolecular disulfide bonds (Appenzeller-Herzog *et al*, 2008; Baker *et al*, 2008). Accordingly, the bulk of purified Ero1α used for *in vitro* assays is in the inactive state (Baker *et al*, 2008), whereas cellular Ero1α is fully activated by DTT at the start of the recovery period. Although PDI is involved in their regulation *in vivo* (Appenzeller-Herzog *et al*, 2008), the protein is not sufficiently reducing to effectively open the stable regulatory disulfide bonds in Ero1α (Baker *et al*, 2008). Addition of GSH to maintain PDI in the reduced form or replacement of PDI with the more reducing thioredoxin more efficiently activated Ero1α and increased the reaction kinetics (Baker *et al*, 2008), but still failed to reproduce the rapid pace of oxidation observed in cells. It therefore appears that the *in vitro* experiments do not faithfully reproduce the situation in the ER where additional factors such as the ionic composition of the solvent (e.g. the levels of calcium), conformational changes in Ero1α induced by an as yet unknown protein, the two N-glycans in Ero1α or the catalyzed metabolic discharge of reaction products such as hydrogen peroxide could have important functions.

PDI is the major, but probably not the only substrate of Ero1

Using acid quenching to trap mixed-disulfide complexes, we identify ERp57 and ERp72 as novel interactors of Ero1α and β. Multiple lines of evidence, however, point to PDI as being the principal interaction partner of Ero1: (1) As opposed to ERp57, PDI is unambiguously required for efficient ER reoxidation following DTT treatment (Fig. 5E-H). (2) Over-expression of Ero1α does not affect the cellular redox state of ERp57 while easily oxidizing PDI (Appenzeller-Herzog *et al*, 2008; Mezghrani *et al*, 2001). (3) PDI**a´** is significantly more resistant than ERp57**a´** towards *in situ* reduction by DTT (Fig. 2). (4) The amount of acid-trapped PDI co-immunoprecipitating with Ero1 is relatively higher than that of ERp57 and ERp72 (Fig. 3). (5) On non-reducing αEro1α Western blots following acid trapping, the mixed disulfide with PDI is the predominant high molecular weight species (Fig. 6B). (6) Depletion and over-expression of PDI, but not of other PDI family members, modulates the formation of the regulatory disulfide bonds in Ero1α ((Appenzeller-Herzog *et al*, 2008); Araki, K. and Nagata, K., personal communication). (7) Among several PDIs that interact with Ero1α in cells, PDI itself is the best substrate in an *in vitro* activity assay and shows the highest affinity for Ero1α (Araki, K. and Nagata, K., personal communication).

Due to the lower prevalence of the ERp57 and ERp72 complexes with Ero1, the functional implications of these interactions are currently unclear. Still, the increased resistance of ERp57 towards *in situ* reduction by DTT as compared to TMX3 (Fig. 2C) and the significant delay in GSSG reformation upon DTT washout in ERp57-/- cells (Fig. 5H) argue that at least under certain conditions, ERp57 can

accept disulfide bonds from Ero1, as has also been observed *in vitro* ((Kulp *et al*, 2006) ; Araki, K. and Nagata, K., personal communication).

We have shown that the PDI–Ero1α/β mixed disulfide in cells at steady state predominantly involves an oxidized form of Ero1 (Fig. 6). It is also worth noting that both PDI and ERp57 interacted with the active-site mutant Ero1α-C94S (data not shown). It was only in DTT-treated cells that formation of the PDI–Ero1α mixed disulfide became strictly dependent on Cys^{94} (Fig. 6C). Due to the typically short-lived nature of a mixed disulfide during thiol-disulfide exchange (see e. g. (Darby and Creighton, 1995)) we reason that the surprisingly abundant Ero1 complexes at steady state do not exclusively represent catalytic reaction intermediates. It thus seems that PDI-related oxidoreductases as well as PDI itself are engaged in as yet uncharacterized mixed-disulfide interactions with Ero1.

Ero1-independent disulfide-bond formation

Murine B-cells depleted of both Ero1 isoforms unexpectedly secrete nearly normal levels of disulfide-bonded immunoglobulins (Zito *et al*, 2010). The results obtained here with ERO1 double mutant cells also provide strong evidence for Ero1-independent generation of disulfides, which may explain the viability of these cells (for a recent review see (Margittai and Banhegyi, 2010)). Although we are currently lacking an explanation for these observations, it is worth noting the different reoxidation kinetics of cellular GSH and of the ER enzyme ERp57 after reduction in Ero1-deficient cells (Figs. 5B and D). In addition, these cells display a disturbed glutathione homeostasis as indicated by a higher $GSSG:GS_{tot}$ (Fig. 5D) and a lower concentration of GS_{tot} (our unpublished observations). The exact nature of Ero1-

independent pathways and their importance in cells harboring an intact Ero1 system will be important topics for future investigation. It is conceivable that such studies will reveal additional important elements of ER redox homeostasis that must be integrated into our current thinking about this process (Fig. 7). Despite all of this, the powerful capability of over-expressed Ero1α to boost GSH reoxidation (Fig. 4C) along with the delayed ER reoxidation in ERO1 double mutant cells (Fig. 5C) clearly indicates a prominent role of Ero1 oxidases in the net generation of disulfides in the mammalian ER.

In conclusion, the present results emphasize the significance of electron flow from PDI to Ero1 for effective ER oxidation in mammalian cells. Moreover, the data indicate that a dynamic equilibrium between Ero1- and GSSG-driven substrate protein oxidation via PDIs constitutes a central element of ER redox control.

Materials and Methods

Recombinant DNA

For generation of the C94S mutant of Ero1α we used pcDNA3.1/Ero1α-myc6his ((Cabibbo *et al*, 2000); a gift from R Sitia, Milan) as a template for QuikChange mutagenesis (Stratagene) using the primer pair 5´-GAATGACATCAGCCAGTCTGGAAGAAGGGACTG-3´ / 5´-CAGTCCCTTCTTCCAGACTGGCTGATGTCATTC-3´. pcDNA3/HA-ERp57SS1 (encoding ERp57 SXXS-CXXC) and pcDNA3/HA-ERp57SS2 (encoding ERp57 CXXC-SXXS) were produced by two consecutive rounds of QuikChange using pcDNA3/HA-ERp57 ((Otsu *et al*, 2006); a gift from R Sitia, Milan) as template. The primer pairs were: First round SS1: 5´-GCCCCCTGGTGTGGACACAGCAAGAGACTTGC-3´ / 5´-GCAAGTCTCTTGCTGTGTCCACACCAGGGGGC-3´. Second round SS1: 5´-GCCCCCTGGTCTGGACACAGCAAGAGACTTGC-3´ / 5´-GCAAGTCTCTTGCTGTGTCCAGACCAGGGGGC-3´. First round SS2: 5´-GCCCCTTGGTGTGGTCATAGCAAGAACCTGGAG-3´ / 5´-CTCCAGGTTCTTGCTATGACCACACCAAGGGGC-3´. Second round SS2: 5´-GCCCCTTGGTCTGGTCATAGCAAGAACCTGGAG-3´ / 5´-CTCCAGGTTCTTGCTATGACCAGACCAAGGGGC-3´.

Cell culture, transfection, drug treatment, and antibodies

The culturing of HEK293, Flp-In TRex-293 cells for doxycyclin-inducible expression of Ero1 variants (or transfected with empty pcDNA5/FRT/TO vector; negative control cells), and HeLa-derived PDI shRNA cells (Ou and Silver, 2006) has been described (Appenzeller-Herzog *et al*, 2008). Immortalized embryonic fibroblasts were prepared from wild-type and Ero1α/Ero1β double mutant mice (Zito *et al*, 2010) and cultivated in Dulbecco's modified eagle medium (4.5 g/l glucose) supplemented with 1% non-essential amino acids and 10% fetal calf serum. 2175+ (ERp57+/+) and 2175- (ERp57-/-) mouse fibroblast cells (Garbi *et al*, 2006) were grown in α-minimal essential medium (Invitrogen) containing 10% fetal calf serum. Transient transfection of cDNA was performed using Lipofectamine 2000 and of siRNA using Lipofectamine RNAiMAX (both Invitrogen). The following siRNAs were used (Qiagen, final concentrations in brackets): Negative control siRNA 1022076 (20 nM) and Hs_ERO1L_5 HP against Ero1α (20 nM). BFA and monensin (both Sigma) were used at a concentration of 5 µg/ml and 100 nM, respectively. For the depletion of glutathione or nascent proteins, the cells were treated with 1 mM BSO for 20 h or 100 µg/ml CHX for 3 h (both Sigma). DTT resistance experiments were carried out using a fresh, aqueous DTT stock solution that was calibrated in 50 mM $NaPO_4$, pH 7.3, 0.1 mM EDTA using 5,5'-dithiobis(2-nitrobenzoic acid) (DTNB ; 1 mM; ε_{412} 14,150 $M^{-1}cm^{-1}$). Cells were then incubated in full growth medium containing defined DTT concentrations for 10 min at 37°C.

The following mouse monoclonal antibodies were used: 9E10 (αmyc, Covance), AC-15 (αactin, Sigma), HA.11 (αHA, Covance), RL90 (αPDI, abcam). The rabbit polyclonal antisera used were as follows: αTMX3 (Haugstetter et al.,

2005), αERp57 (a gift from A Helenius, Zürich), SPA-890 (αPDI, Stressgen), SPS-720 (αERp72, Stressgen), αEro1α (D5, a gift from I. Braakman, Utrecht).

Assays for the in vivo redox states of PDIs and glutathione

Protocols for alkylation of originally oxidized cysteines with methoxy polyethylene glycol 5000 maleimide (mPEG-mal) or AMS have been published (Appenzeller-Herzog and Ellgaard, 2008a). The cellular GSSG:GSH ratio was measured using a DTNB/glutathione reductase recycling assay as previously described (Appenzeller-Herzog *et al*, 2008).

In situ acid-trapping, immunoprecipitation and concanavalin A (ConA)-precipitation

Cells induced with 1 ⌈g/ml doxycyclin for 24 h, pulsed with ^{35}S-methionine (Perkin Elmer) for 1 h in the presence of doxycyclin, and chased for 1 h with 10 mM cold methionine in the presence or absence of 100 ⌈g/ml CHX were washed with cold PBS, covered with 10% TCA and incubated on ice for 15 min. The precipitated cell material was then scraped from the culture dish with a rubber policeman, pelleted at 20,000 x g at 4°C for 15 min and the pellet covered with a solution containing 58 mM Tris/HCl pH 7, 27% dimethyl sulfoxide, 7.3% glycerol, 1.5 % SDS, 15 mM NEM, 0.2 mM phenylmethylsulfonylfluoride, 0.1% bromcresol purple. After neutralization of the supernatant by dropwise addition of 1 M Tris/Cl, pH 8 until the solution turned purple, the pellet was solubilized using a microsonicator equipped with a 0.5 mm sonotrode (Hielscher Ultrasound Technology, Teltow, Germany) followed by incubation at room temperature for 1 h. Ten sample volumes of cold 30 mM Tris/HCl,

pH 8.1, 100 mM NaCl, 5 mM EDTA, and 2% Triton X-100 were then added, and the lysate processed for ⟨myc immunoprecipitation as described previously (Appenzeller-Herzog and Ellgaard, 2008a). Immunoprecipitates were analyzed by reducing or non-reducing SDS-PAGE and Western blotting, followed by exposure of the Western blot membrane to a phosphor screen (GE Healthcare) for autoradiography. Ahead of precipitation using ConA-sepharose (Sigma), SDS-lysates of TCA-pellets were mixed with ten volumes of 100 mM $NaPO_4$, pH 6.8, 1.5% TX-100.

DTT washout assays

For measuring the recovery of cellular GSSG levels after DTT treatment, the cells were grown in 10 cm dishes and incubated for 5 min in medium containing 10 mM DTT. The cell monolayers were then quickly washed twice with 5 ml of PBS at room temperature (a step taking ~30 s) and, for oxidative recovery, covered again with PBS (defined as the 0 s time point). The reaction was stopped by the removal of PBS and the addition of ice-cold 1% sulfosalicylic acid.

For visualization of the TMX3 and ERp57 redox states upon DTT washout, the cells were grown on plastic coverslips (diameter ~30 mm, placed in a 6 well dish) that had been excised from 35 mm cell culture dishes and sterilized by UV light. DTT treatment (1 mM) was for 5 min at 37°C in growth medium. Subsequently, the coverslips were picked with forceps, drained on a paper towel, consecutively dipped into three beakers containing 37°C PBS (for ~1 s each) and into another warm PBS bathing solution for the indicated periods. For the 0 s time point, this last incubation step was omitted. Oxidative recovery was terminated by dipping the coverslips into

ice-cold PBS containing 20 mM NEM. After a 20 min incubation in NEM buffer on ice, the cells were further processed for AMS alkylation.

Densitometric analyses

To evaluate the results obtained by the AMS assay the ratios of oxidized to reduced species on αTMX3 and αERp57 Western blots were analyzed by densitometry using the ImageJ software (available at rsbweb.nih.gov/ij). Of note, the steady-state redox states of both TMX3 and ERp57 varied between individual experiments, which likely reflected physiological fluctuations rather than low reliability of the AMS assay (see the diamide control lanes). To normalize for these variations we therefore expressed the oxidized fractions as percentage of the oxidized fraction in the steady-state lane of the same experiment.

Acknowledgements

We thank Sandra Abel Nielsen and Nicole Beuret for excellent technical assistance, Mirko Lukic for the production of plastic coverslips, Roberto Sitia, Ineke Braakman, Jonathan Silver, Günter J. Hämmerling, and Ari Helenius for providing reagents, and the members of the Ellgaard laboratory and Jakob R. Winther for helpful discussions and critical reading of the manuscript. Funding obtained from the Swiss National Science Foundation (SNSF), the Böhringer Ingelheim Foundation, the Novartis Stiftung, Carlsbergfondet, Novo Nordisk Fonden, the European Molecular Biology Organization, and the National Institutes of Health is gratefully acknowledged. C. A.-H. is an independent ambizione fellow of the SNSF.

References

Appenzeller-Herzog C, Ellgaard L (2008a) In vivo reduction-oxidation state of protein disulfide isomerase: the two active sites independently occur in the reduced and oxidized forms. *Antioxid Redox Signal* **10:** 55-64

Appenzeller-Herzog C, Ellgaard L (2008b) The human PDI family: versatility packed into a single fold. *Biochim Biophys Acta* **1783:** 535-548

Appenzeller-Herzog C, Riemer J, Christensen B, Sorensen ES, Ellgaard L (2008) A novel disulphide switch mechanism in Ero1alpha balances ER oxidation in human cells. *EMBO J* **27:** 2977-2987

Baker KM, Chakravarthi S, Langton KP, Sheppard AM, Lu H, Bulleid NJ (2008) Low reduction potential of Ero1alpha regulatory disulphides ensures tight control of substrate oxidation. *EMBO J* **27:** 2988-2997

Banhegyi G, Lusini L, Puskas F, Rossi R, Fulceri R, Braun L, Mile V, di Simplicio P, Mandl J, Benedetti A (1999) Preferential transport of glutathione versus glutathione disulfide in rat liver microsomal vesicles. *J Biol Chem* **274:** 12213-12216

Barzilay E, Ben-Califa N, Hirschberg K, Neumann D (2005) Uncoupling of brefeldin a-mediated coatomer protein complex-I dissociation from Golgi redistribution. *Traffic* **6:** 794-802

Bass R, Ruddock LW, Klappa P, Freedman RB (2004) A major fraction of endoplasmic reticulum-located glutathione is present as mixed disulfides with protein. *J Biol Chem* **279:** 5257-5262

Benham AM, Cabibbo A, Fassio A, Bulleid N, Sitia R, Braakman I (2000) The CXXCXXC motif determines the folding, structure and stability of human Ero1-Lalpha. *EMBO J* **19:** 4493-4502

Cabibbo A, Pagani M, Fabbri M, Rocchi M, Farmery MR, Bulleid NJ, Sitia R (2000) ERO1-L, a human protein that favors disulfide bond formation in the endoplasmic reticulum. *J Biol Chem* **275:** 4827-4833

Chakravarthi S, Bulleid NJ (2004) Glutathione is required to regulate the formation of native disulfide bonds within proteins entering the secretory pathway. *J Biol Chem* **279:** 39872-39879

Chakravarthi S, Jessop CE, Bulleid NJ (2006) The role of glutathione in disulphide bond formation and endoplasmic-reticulum-generated oxidative stress. *EMBO Rep* **7:** 271-275

Cuozzo JW, Kaiser CA (1999) Competition between glutathione and protein thiols for disulphide-bond formation. *Nat Cell Biol* **1:** 130-135

Darby NJ, Creighton TE (1995) Characterization of the active site cysteine residues of the thioredoxin-like domains of protein disulfide isomerase. *Biochemistry* **34:** 16770-16780

Dias-Gunasekara S, Gubbens J, van Lith M, Dunne C, Williams JA, Kataky R, Scoones D, Lapthorn A, Bulleid NJ, Benham AM (2005) Tissue-specific expression and dimerization of the endoplasmic reticulum oxidoreductase Ero1beta. *J Biol Chem* **280:** 33066-33075

Dutton RJ, Boyd D, Berkmen M, Beckwith J (2008) Bacterial species exhibit diversity in their mechanisms and capacity for protein disulfide bond formation. *Proc Natl Acad Sci U S A* **105:** 11933-11938

Enyedi B, Varnai P, Geiszt M (2010) Redox State of the Endoplasmic Reticulum Is Controlled by Ero1L-alpha and Intraluminal Calcium. *Antioxid Redox Signal* **in press:** doi:10.1089/ars.2009.2880

Frand AR, Kaiser CA (1998) The ERO1 gene of yeast is required for oxidation of protein dithiols in the endoplasmic reticulum. *Mol Cell* **1:** 161-170

Frand AR, Kaiser CA (1999) Ero1p oxidizes protein disulfide isomerase in a pathway for disulfide bond formation in the endoplasmic reticulum. *Mol Cell* **4:** 469-477

Frickel EM, Frei P, Bouvier M, Stafford WF, Helenius A, Glockshuber R, Ellgaard L (2004) ERp57 is a multifunctional thiol-disulfide oxidoreductase. *J Biol Chem* **279:** 18277-18287

Garbi N, Tanaka S, Momburg F, Hammerling GJ (2006) Impaired assembly of the major histocompatibility complex class I peptide-loading complex in mice deficient in the oxidoreductase ERp57. *Nat Immunol* **7:** 93-102

Gilady SY, Bui M, Lynes EM, Benson MD, Watts R, Vance JE, Simmen T (2010) Ero1alpha requires oxidizing and normoxic conditions to localize to the mitochondria-associated membrane (MAM). *Cell Stress Chaperones* **in press:** doi:10.1007/s12192-12010-10174-12191

Gross E, Sevier CS, Heldman N, Vitu E, Bentzur M, Kaiser CA, Thorpe C, Fass D (2006) Generating disulfides enzymatically: reaction products and electron acceptors of the endoplasmic reticulum thiol oxidase Ero1p. *Proc Natl Acad Sci U S A* **103:** 299-304

Hansen RE, Roth D, Winther JR (2009) Quantifying the global cellular thiol-disulfide status. *Proc Natl Acad Sci U S A* **106:** 422-427

Hatahet F, Ruddock LW (2009) Protein Disulfide Isomerase: A Critical Evaluation of Its Function in Disulfide Bond Formation. *Antioxid Redox Signal* **11:** 2807-2850

Haugstetter J, Blicher T, Ellgaard L (2005) Identification and characterization of a novel thioredoxin-related transmembrane protein of the endoplasmic reticulum. *J Biol Chem* **280:** 8371-8380

Haugstetter J, Maurer MA, Blicher T, Pagac M, Wider G, Ellgaard L (2007) Structure-function analysis of the endoplasmic reticulum oxidoreductase TMX3 reveals interdomain stabilization of the N-terminal redox-active domain. *J Biol Chem* **282:** 33859-33867

Jessop CE, Bulleid NJ (2004) Glutathione directly reduces an oxidoreductase in the endoplasmic reticulum of mammalian cells. *J Biol Chem* **279:** 55341-55347

Jessop CE, Watkins RH, Simmons JJ, Tasab M, Bulleid NJ (2009) Protein disulphide isomerase family members show distinct substrate specificity: P5 is targeted to BiP client proteins. *J Cell Sci* **122:** 4287-4295

Karala AR, Lappi AK, Saaranen M, Ruddock LW (2009) Efficient Peroxide Mediated Oxidative Refolding of a Protein at Physiological Ph and Implications for Oxidative Folding in the Endoplasmic Reticulum. *Antioxid Redox Signal* **11:** 963-970

Kulp MS, Frickel EM, Ellgaard L, Weissman JS (2006) Domain architecture of protein-disulfide isomerase facilitates its dual role as an oxidase and an isomerase in Ero1p-mediated disulfide formation. *J Biol Chem* **281:** 876-884

Li G, Mongillo M, Chin KT, Harding H, Ron D, Marks AR, Tabas I (2009) Role of ERO1-alpha-mediated stimulation of inositol 1,4,5-triphosphate receptor

activity in endoplasmic reticulum stress-induced apoptosis. *J Cell Biol* **186:** 783-792

Lyles MM, Gilbert HF (1991) Catalysis of the oxidative folding of ribonuclease A by protein disulfide isomerase: dependence of the rate on the composition of the redox buffer. *Biochemistry* **30:** 613-619

Malhotra JD, Kaufman RJ (2007) Endoplasmic reticulum stress and oxidative stress: a vicious cycle or a double-edged sword? *Antioxid Redox Signal* **9:** 2277-2293

Marciniak SJ, Yun CY, Oyadomari S, Novoa I, Zhang Y, Jungreis R, Nagata K, Harding HP, Ron D (2004) CHOP induces death by promoting protein synthesis and oxidation in the stressed endoplasmic reticulum. *Genes & development* **18:** 3066-3077

Margittai E, Banhegyi G (2010) Oxidative folding in the endoplasmic reticulum: Towards a multiple oxidant hypothesis? *FEBS Lett* **in press:** doi:10.1016/j.febslet.2010.1005.1055

Merksamer PI, Trusina A, Papa FR (2008) Real-time redox measurements during endoplasmic reticulum stress reveal interlinked protein folding functions. *Cell* **135:** 933-947

Mezghrani A, Fassio A, Benham A, Simmen T, Braakman I, Sitia R (2001) Manipulation of oxidative protein folding and PDI redox state in mammalian cells. *EMBO J* **20:** 6288-6296

Molteni SN, Fassio A, Ciriolo MR, Filomeni G, Pasqualetto E, Fagioli C, Sitia R (2004) Glutathione limits Ero1-dependent oxidation in the endoplasmic reticulum. *J Biol Chem* **279:** 32667-32673

Nadanaka S, Okada T, Yoshida H, Mori K (2007) Role of disulfide bridges formed in the luminal domain of ATF6 in sensing endoplasmic reticulum stress. *Mol Cell Biol* **27:** 1027-1043

Otsu M, Bertoli G, Fagioli C, Guerini-Rocco E, Nerini-Molteni S, Ruffato E, Sitia R (2006) Dynamic retention of Ero1alpha and Ero1beta in the endoplasmic reticulum by interactions with PDI and ERp44. *Antioxid Redox Signal* **8:** 274-282

Ou W, Silver J (2006) Role of protein disulfide isomerase and other thiol-reactive proteins in HIV-1 envelope protein-mediated fusion. *Virology* **350:** 406-417

Pagani M, Fabbri M, Benedetti C, Fassio A, Pilati S, Bulleid NJ, Cabibbo A, Sitia R (2000) Endoplasmic reticulum oxidoreductin 1-lbeta (ERO1-Lbeta), a human gene induced in the course of the unfolded protein response. *J Biol Chem* **275:** 23685-23692

Pollard MG, Travers KJ, Weissman JS (1998) Ero1p: a novel and ubiquitous protein with an essential role in oxidative protein folding in the endoplasmic reticulum. *Mol Cell* **1:** 171-182

Roth D, Lynes E, Riemer J, Hansen HG, Althaus N, Simmen T, Ellgaard L (2010) A di-arginine motif contributes to the ER localization of the type I transmembrane ER oxidoreductase TMX4. *Biochem J* **425:** 195-205

Saaranen M, Karala AR, Lappi AK, Ruddock LW (2010) The Role of Dehydroascorbate in Disulfide Bond Formation. *Antioxid Redox Signal* **12:** 15-25

Santos CX, Tanaka LY, Wosniak J, Laurindo FR (2009) Mechanisms and implications of reactive oxygen species generation during the unfolded protein

response: roles of endoplasmic reticulum oxidoreductases, mitochondrial electron transport, and NADPH oxidase. *Antioxid Redox Signal* **11:** 2409-2427

Sevier CS, Kaiser CA (2008) Ero1 and redox homeostasis in the endoplasmic reticulum. *Biochim Biophys Acta* **1783:** 549-556

Sevier CS, Qu H, Heldman N, Gross E, Fass D, Kaiser CA (2007) Modulation of cellular disulfide-bond formation and the ER redox environment by feedback regulation of Ero1. *Cell* **129:** 333-344

Singh AK, Bhattacharyya-Pakrasi M, Pakrasi HB (2008) Identification of an atypical membrane protein involved in the formation of protein disulfide bonds in oxygenic photosynthetic organisms. *J Biol Chem* **283:** 15762-15770

Thorpe C, Kodali VK (2010) Oxidative Protein Folding and the Quiescin-sulfhydryl Oxidase Family of Flavoproteins. *Antioxid Redox Signal* **in press:** doi:10.1089/ars.2010.3098

Tien AC, Rajan A, Schulze KL, Ryoo HD, Acar M, Steller H, Bellen HJ (2008) Ero1L, a thiol oxidase, is required for Notch signaling through cysteine bridge formation of the Lin12-Notch repeats in Drosophila melanogaster. *J Cell Biol* **182:** 1113-1125

Tu BP, Ho-Schleyer SC, Travers KJ, Weissman JS (2000) Biochemical basis of oxidative protein folding in the endoplasmic reticulum. *Science* **290:** 1571-1574

Wajih N, Hutson SM, Wallin R (2007) Disulfide-dependent protein folding is linked to operation of the vitamin K cycle in the endoplasmic reticulum. A protein disulfide isomerase-VKORC1 redox enzyme complex appears to be responsible for vitamin K1 2,3-epoxide reduction. *J Biol Chem* **282:** 2626-2635

Wang L, Li SJ, Sidhu A, Zhu L, Liang Y, Freedman RB, Wang CC (2008) Reconstitution of human Ero1-La/protein disulfide isomerase oxidative folding pathway in vitro: Position-dependent differences in role between the A and A' domains of protein disulfide isomerase. *J Biol Chem* **284:** 199-206

Yang Y, Song Y, Loscalzo J (2007) Regulation of the protein disulfide proteome by mitochondria in mammalian cells. *Proc Natl Acad Sci U S A* **104:** 10813-10817

Zapun A, Darby NJ, Tessier DC, Michalak M, Bergeron JJ, Thomas DY (1998) Enhanced catalysis of ribonuclease B folding by the interaction of calnexin or calreticulin with ERp57. *J Biol Chem* **273:** 6009-6012

Zito E, Chin KT, Blais J, Harding HP, Ron D (2010) ERO1-beta, a pancreas-specific disulfide oxidase, promotes insulin biogenesis and glucose homeostasis. *J Cell Biol* **188:** 821-832

Figure Legends

Fig. 1: Vesicular transport, glutathione concentration, and protein translocation only moderately influence ER redox homeostasis

(A) HEK293 cells pre-treated with BFA/mon for 0.5 h or left untreated were incubated with 5 mM diamide (dia) for 5 min, washed twice with PBS and incubated in the same buffer for 0, 5, 10, or 15 min (wo, washout). BFA/mon was present throughout the time course. For comparison, steady-state samples ± treatment with BFA/mon for 0.5 h were included. The reactions were stopped by rinsing the cells in ice-cold PBS containing 20 mM NEM, and the redox distributions of TMX3 and ERp57 visualized by Western blotting (WB) after differential alkylation with NEM and AMS. The mobility of the oxidized (ox) and reduced (red) forms of TMX3 and ERp57 are indicated.

(B) Recovery of the TMX3 redox ratio assessed by densitometry in BFA/mon-treated and control cells as shown in panel (A) (n=3, mean ± SD).

(C) The redox states of TMX3 and ERp57 in HEK293 cells depleted of glutathione (using BSO) or nascent proteins (using CHX). Treatment with BSO reduced cellular glutathione levels to 20% of control (data not shown). Oxidized fractions (%) as determined by densitometry are indicated. Lanes labeled with dia represent oxidized control lanes using diamide-treated cell lysates. The hairlines indicate where intervening lanes have been removed. Results are representative of three independent experiments.

Fig. 2: *In vivo* DTT resistance of PDI, TMX3, and ERp57

(A) HEK293 cells were treated with the indicated concentrations of DTT, and the *in vivo* redox state of the two active sites in PDI (**a** and **a´**) determined by immunoprecipitation (IP) of ^{35}S-labeled and mPEG-mal-modified PDI. Samples completely reduced with DTT and TCEP, or oxidized with diamide (dia) served as mobility markers. The contrast-enhancement of the region marked by the rectangle more clearly shows the different behaviour of the two semi-oxidized forms of PDI (**a** domain oxidized / **a´** domain reduced (**a**-ox); **a** domain reduced / **a´** domain oxidized (**a´**-ox)), for which we have previously determined the relative mobility (Appenzeller-Herzog and Ellgaard, 2008a). One of two independent experiments with equal outcome is shown. Red, both active sites reduced; ox, both active sites oxidized; asterisks, reduced PDI modified with mPEG-mal on its non-catalytic cysteines (Appenzeller-Herzog and Ellgaard, 2008a).

(B) After treatment of HEK293 cells with the indicated concentrations of DTT, the *in vivo* redox states of TMX3 and ERp57 were determined as in Fig. 1A. The mobilities of the oxidized (ox) and reduced (red) species, as verified by control samples using lysates from diamide- or DTT (10^4 μM)-treated cells, are marked.

(C) Densitometric analysis of (B) (n=3, mean ± SD).

Fig. 3: Mixed-disulfide interactions of PDIs with Ero1α/β

Doxycyclin-induced and *in situ* acid-trapped negative control, Ero1αmyc6his, and Ero1βmyc6his cells were subjected to αmyc immunoprecipitation (IP) followed by reducing (R) or non-reducing (NR) SDS-PAGE and Western blot (WB) analysis using

αPDI (A), αERp57 (B), αERp72 (C), or αTMX3 (D). The ^{35}S-signal recorded by phosphorimaging of one of the membranes is shown in Fig. S2B. As positive controls for Western blotting, 1% of the Ero1αmyc6his lysate (1% of total) as well as reduced and non-labelled HEK293 lysate (cold lysate) were loaded in lanes 1 and 2. The results are representative of two independent experiments. Filled arrowheads, monomeric PDIs; open arrowheads, dimeric mixed-disulfide complexes of PDIs with Ero1 (the precise mobility of which is unclear in the case of ERp72; indicated by a vertical line); asterisks, potential mixed-disulfide complexes of PDIs with Ero1α dimers; X, background bands.

Fig. 4: ER reoxidation after DTT treatment is fast and affected by exogenous Ero1

(A) Intracellular levels of GSSG and GS_{tot} were recorded from DTT-treated HEK293 cells after washout of the reductant for 0 s, 10 s, 30 s, 1 min, 3 min, 5 min, or 20 min. The GSSG:GS_{tot} ratio is expressed as percentage of the steady-state value that was independently measured (mean ± SD, n=8, for individual experiments see Fig. S3A).

(B) Negative control cells were grown on plastic coverslips, treated with or without doxycyclin (dox) for 24 h, and left untreated (-) or incubated with DTT. After 0, 5, 10, or 20 s of DTT washout (wo), the cells were processed for AMS-alkylation and Western blotting (WB) using αTMX3 or αERp57. Ox, oxidized species; red, reduced species; dia, oxidized control lane using diamide-treated cells.

(C-F) DTT washout assays followed by the determination of cellular levels of GSSG and GS_{tot} after 0, 10, 60, or 300 s using Ero1⟨myc6his (C), Ero1βmyc6his (D), Ero1⟨myc6his-C131A (E), and Ero1⟨myc6his-C394A (F) cells cultured for 24 h with

or without (control) the addition of doxycyclin (mean ± SD, two independent experiments each performed in triplet, Figs. S3D-G). *, $p < 0.05$; **, $p < 0.01$; ***, $p < 0.001$ (Student's *t*-test). Notice the different scaling on the y-axis in the individual panels.

Fig. 5: Rapid oxidative recovery of the ER depends on Ero1 and PDI

(A) Lysates of wild-type (+/+;+/+) or double mutant (i/i;i/i) mouse embryonic fibroblasts (MEFs) were analyzed by reducing (R) or non-reducing (NR) SDS-PAGE and αEro1〈 Western blotting after ConA-precipitation. The gel mobilities of the three known redox forms of Ero1α (R, OX1, OX2) are indicated.

(B) Redox state analysis of ERp57 following DTT washout using wild-type (+/+;+/+) or double mutant (i/i;i/i) MEFs. The experiment was performed as in Figs. 4B and S4B except that oxidative recovery was allowed for longer periods. Open arrowheads indicate the delayed formation of oxidized ERp57 in double mutant cells.

(C) Densitometric analysis of (B) (n=3, mean ± SD).

(D) GSSG:GS_{tot} was determined in wild-type (+/+;+/+) or double mutant (i/i;i/i) MEFs at the indicated intervals after DTT washout (mean ± SD, three independent experiments each performed in triplet, Fig. S4D). For unknown reasons, GSSG:GS_{tot} rises above the steady-state value after 300 s of oxidative recovery in wild-type cells. The GSSG:GS_{tot} ratios in wild-type and double mutant MEFs at steady state are shown in the inset (n=12).

(E) Redox state analysis of TMX3 and ERp57 following DTT washout performed as in Fig. 4B, but using PDI shRNA clones 5-1 (control cells) and 4-1 (PDI knockdown

(kd) cells). Open arrowheads indicate the delayed formation of oxidized TMX3/ERp57 upon knockdown of PDI.

(F) Densitometric analysis of (D) (n=3, mean ± SD).

(G and H) The oxidative recovery of GSSG:GS_{tot} following DTT washout was determined as in Fig. 4C using clone 5-1 (control) and clone 4-1 (PDI kd) cells (G) or 2175^{+} (control) and 2175^{-} (ERp57 ko) cells (H) (mean ± SD, two independent experiments each performed in triplet, Fig. S4E and F). For unknown reasons, GSSG:GS_{tot} rises above the steady-state value after 300 s of oxidative recovery in 2175^{+} and 2175^{-} cells. *, $p < 0.05$; **, $p < 0.01$; ***, $p < 0.001$ (Student's *t*-test).

Fig. 6: Upon reductive challenge, activated Ero1α rapidly reacts with PDI

(A) Co-immunoprecipitation performed in analogy to the experiment presented in Fig. 3 except that, where indicated, cells were treated with DTT ahead of TCA lysis. A phosphoimager scan (IP: αmyc (Ero1)) and a Western blot (WB) using αPDI are shown. The mobility differences between the Ero1–PDI mixed-disulfide complexes (Ero1+PDI) under steady-state conditions (OX.) and upon DTT-mediated reduction (RED.) are marked. For unknown reasons, the intensity of WB detection of Ero1+PDI did not reflect the relative intensities observed by phosphorimaging. Note that an NEM- and redox state-dependent mobility shift of Ero1α in reducing SDS-PAGE (compare lanes 2 and 3; see also panel B) has been reported previously (Benham *et al*, 2000). The result is representative of two independent experiments. Filled arrowhead, monomeric PDI; asterisks, Ero1α/βmyc6his–ERp57 mixed-disulfide complex (inferred from Fig. S5); X, background band.

(B) TCA pellets from HEK293 cells incubated with DTT or left untreated were solubilized/neutralized in the presence of NEM, and Ero1α was precipitated from the lysate using ConA-sepharose (Benham *et al*, 2000). The precipitate was boiled under reducing (R) or non-reducing (NR) conditions and analyzed by αPDI Western blotting (WB, left panel). After stripping, the membrane was probed with αEro1α (right panel). The mobilities of PDI, the known monomeric redox forms of Ero1α (R, OX1, OX2; visible upon contrast-enhancement), and of the Ero1α+PDI complex (both RED. and OX.) are indicated. Results are representative of three independent experiments. Asterisk, potential mixed-disulfide complex of PDI with an Ero1α dimer; double asterisk, unidentified, DTT-resistant mixed-disulfide complex.

(C) Phosphorimager scan of a co-immunoprecipitation experiment performed as in panel (A). In addition to doxycyclin-induced Ero1αmyc6his cells (dox), HEK293 transiently transfected (cDNA) with pcDNA3/Ero1α or pcDNA3/Ero1α-C94S were used. For unknown reasons, the monomeric form of transiently transfected Ero1αmyc6his is more exposed than stably transfected Ero1αmyc6his to DTT-mediated reduction (as indicated by enhanced conversion of OX2 into more reduced, slower migrating forms). The result is representative of two independent experiments. Asterisk, Ero1αmyc6his–ERp57 mixed-disulfide complex (compare Fig. S5).

Fig. 7: Model for glutathione-buffered ER redox homeostasis

Graphical depiction of two disulfide relay pathways that both lead to the oxidation of nascent proteins (substrate) in the ER. (A) In the Ero1α-driven oxidation pathway for *de novo* disulfide formation, oxidizing equivalents are transferred from O_2 to Ero1α

that in turn oxidizes PDI. The byproduct H_2O_2 can also oxidize PDI yielding two molecules of H_2O (Karala *et al*, 2009). A potential *in vivo* catalyst of this reaction remains to be identified (question mark). Abundant levels of reduced PDI keep Ero1α in an active state (green arrow) (Appenzeller-Herzog *et al*, 2008). Being the main substrate of Ero1α, disulfides are passed on primarily to PDI, but other PDI-family members (PDIs) may also participate to some extent in this pathway. GSH competes with substrate for reaction with oxidized PDI, resulting in the formation of GSSG. (B) GSSG-driven oxidation of reduced PDIs (yellow arrows) will be prominent when ER GSSG is abundant, which will also promote shutdown of Ero1α due to low availability of reduced PDI. Like for the Ero1α-driven oxidation pathway, the PDIs will then oxidize substrate proteins (blue arrows). The interplay between the two pathways depends on the redox state of the glutathione redox couple in the ER. For instance, during oxidative recovery after DTT treatment *de novo* disulfide generation is dominant immediately following DTT washout. However, as GSSG levels rise, the GSSG-driven oxidation pathway will become increasingly more prominent until homeostasis is reinstalled. For simplicity, the scheme only illustrates the net flow of oxidizing equivalents onto substrate and excludes the reduction of e.g. aberrantly disulfide-bonded substrates by PDIs. Likewise, the direct reaction of GSSG with reduced substrates that results in glutathionylated substrates (Bass *et al*, 2004; Hansen *et al*, 2009) has been omitted. The model does not account for the contribution to ER thiol-disulfide homeostasis by Ero1-independent pathway(s) since the exact nature of these is not yet known. Red, reduced; ox, oxidized.

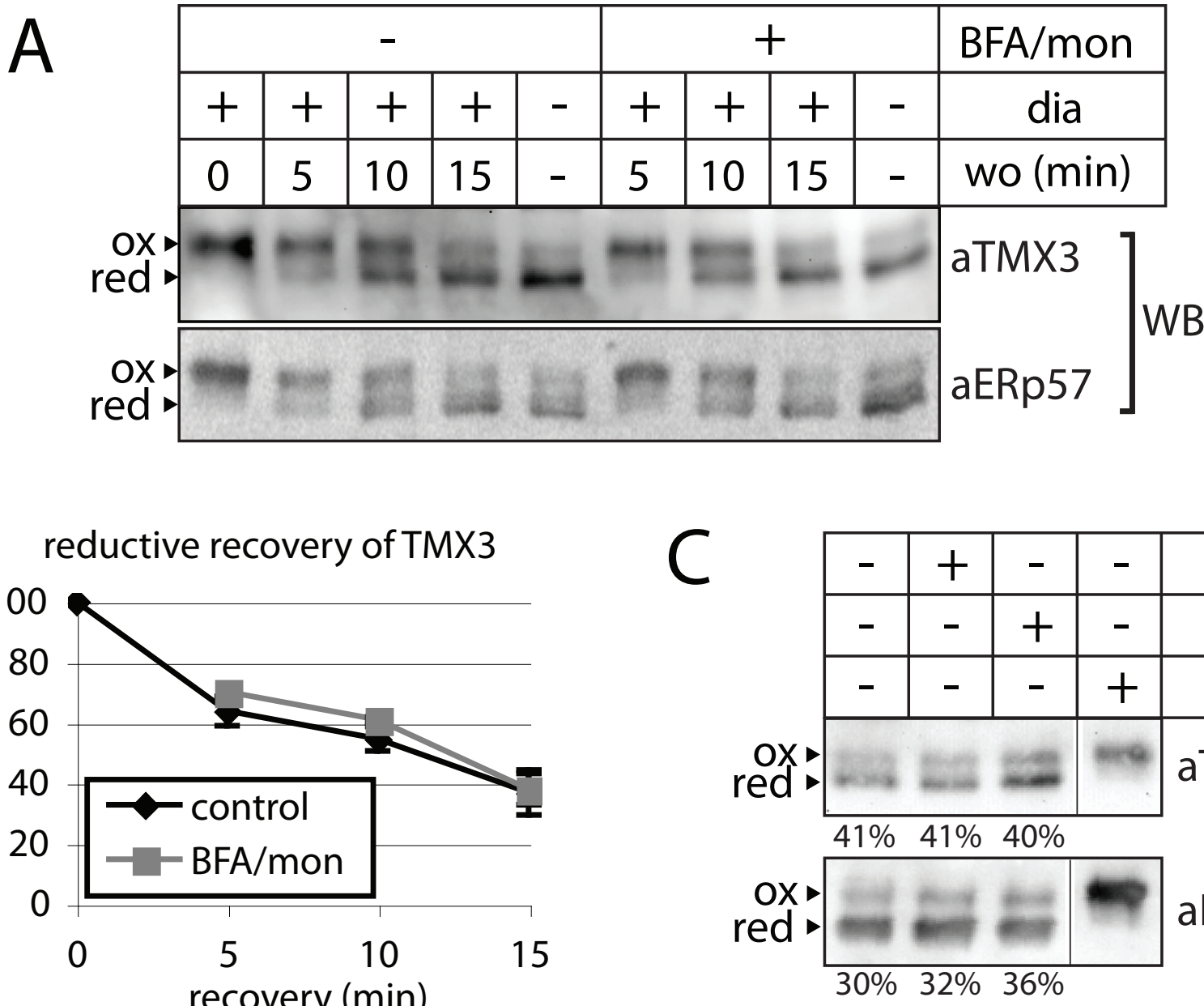

Appenzeller-Herzog et al. Figure 1

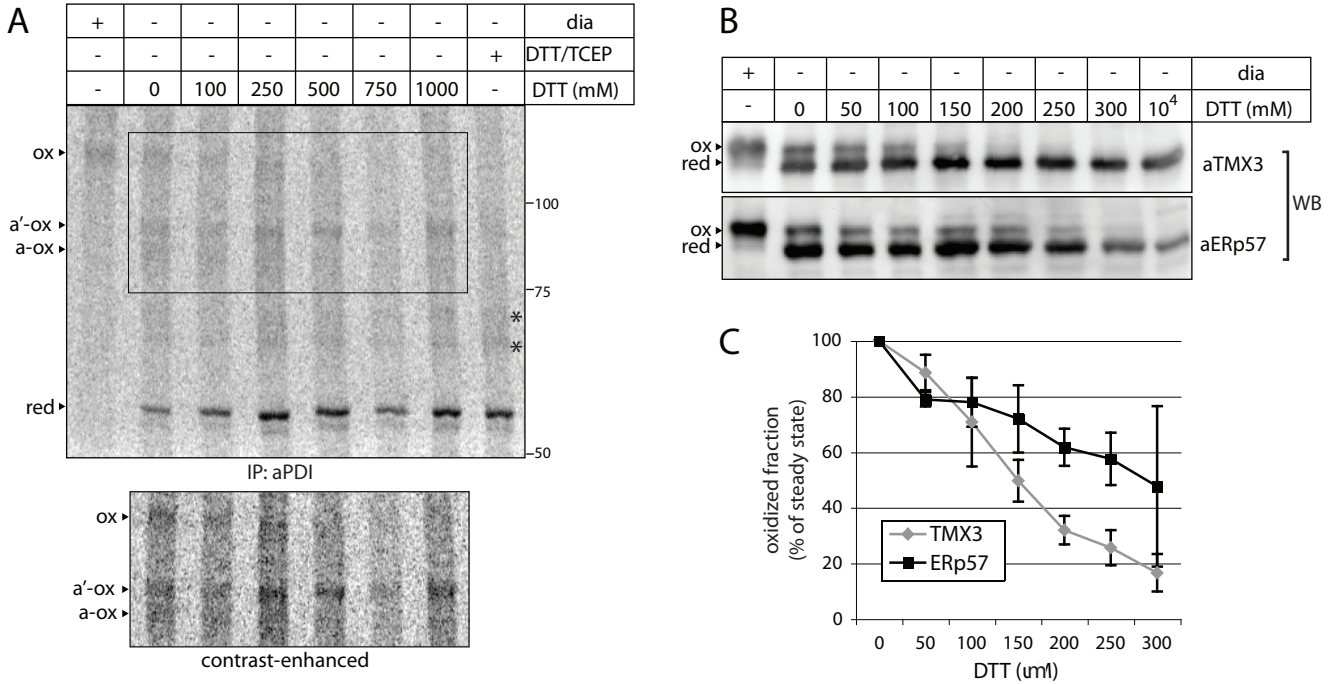

Appenzeller-Herzog et al. Figure 2

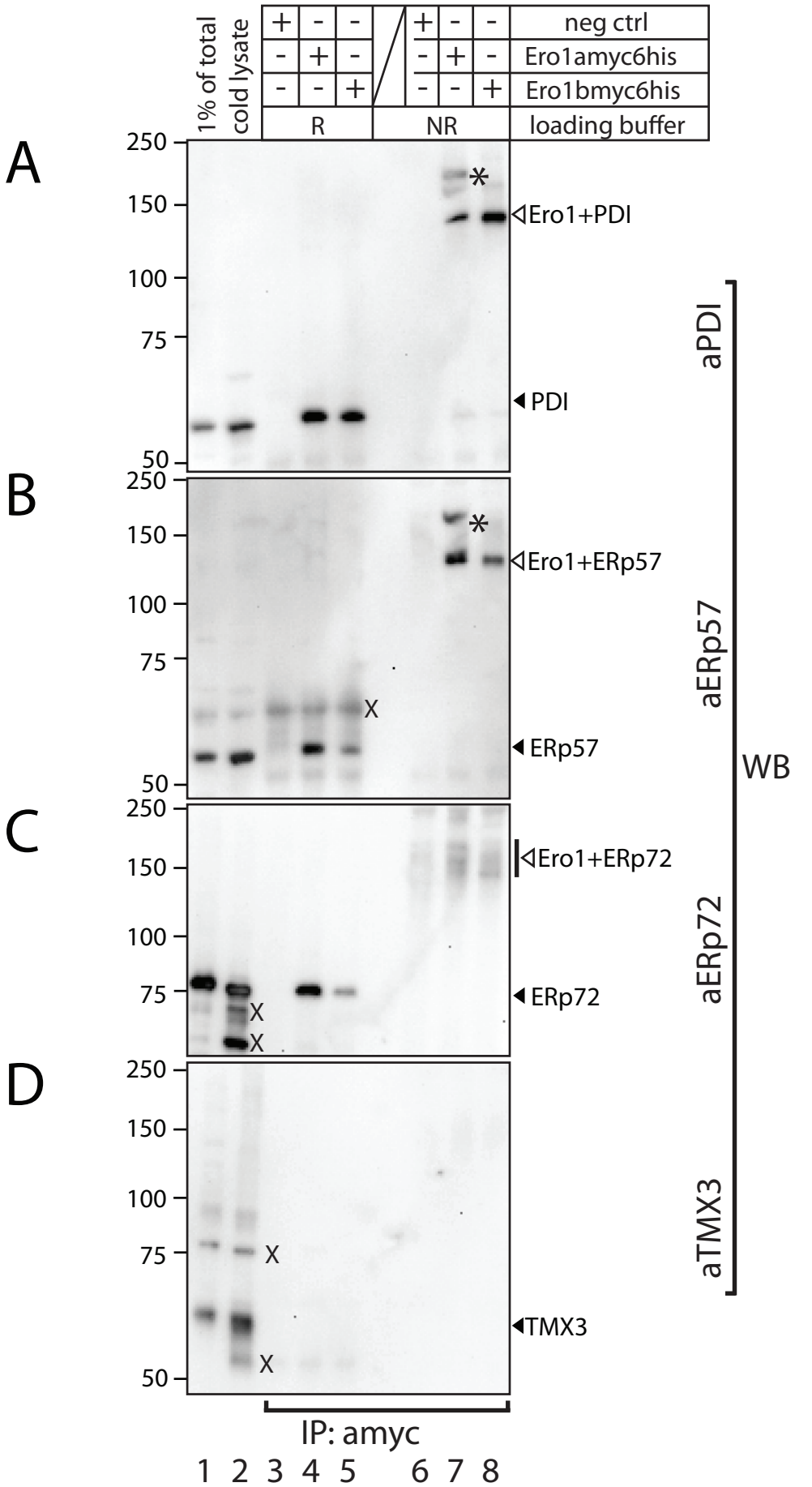

Appenzeller-Herzog et al. Figure 3

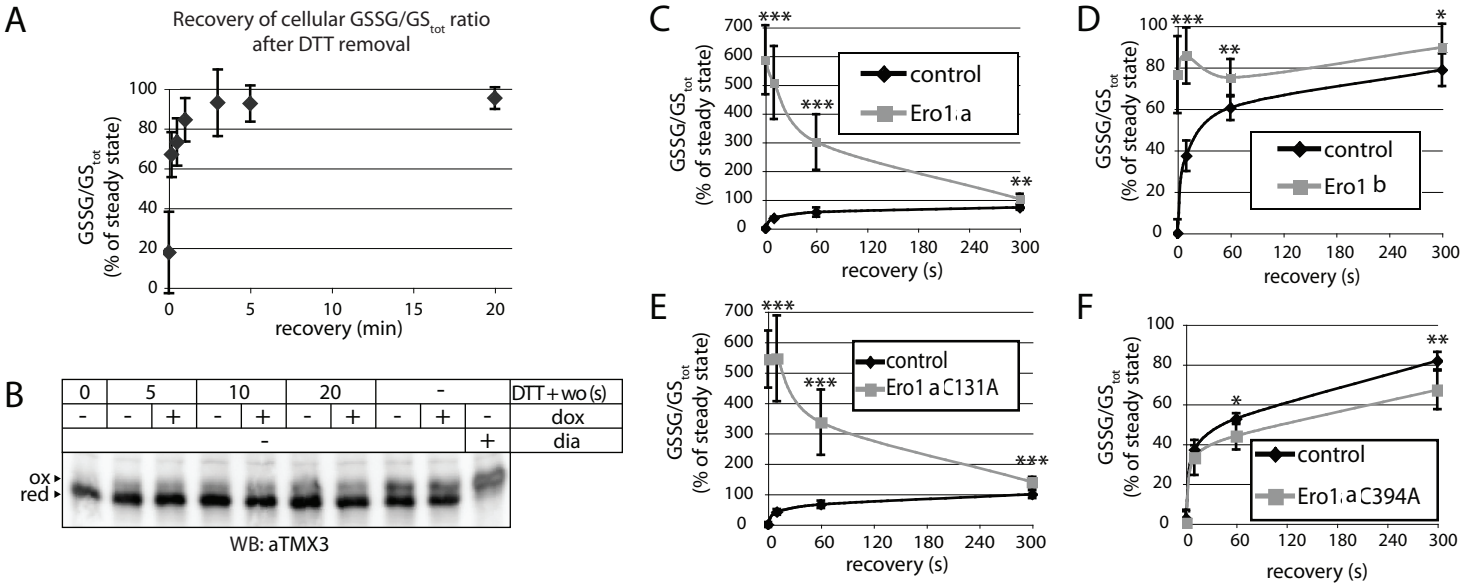

Appenzeller-Herzog et al. Figure 4

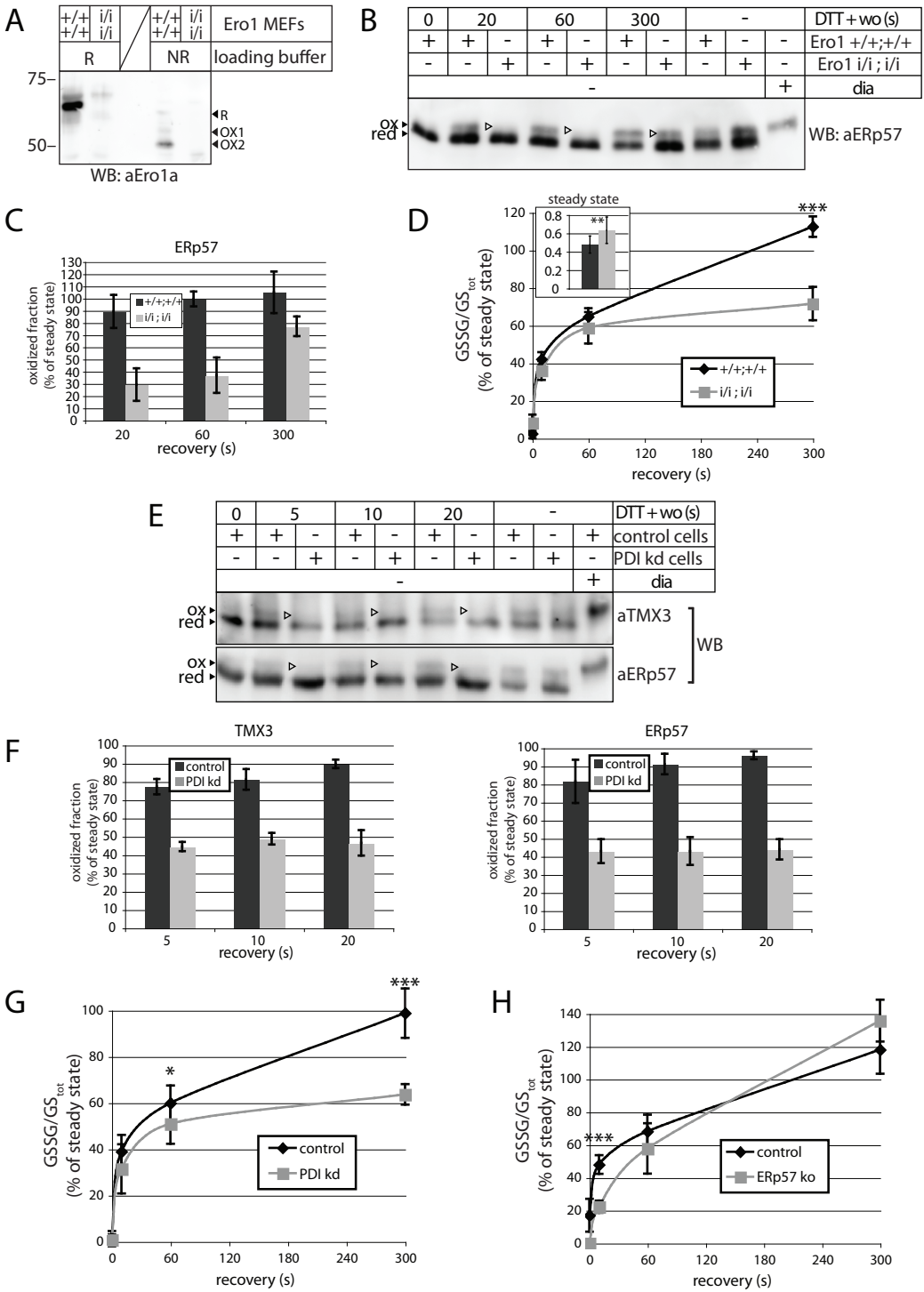

Appenzeller-Herzog et al. Figure 5

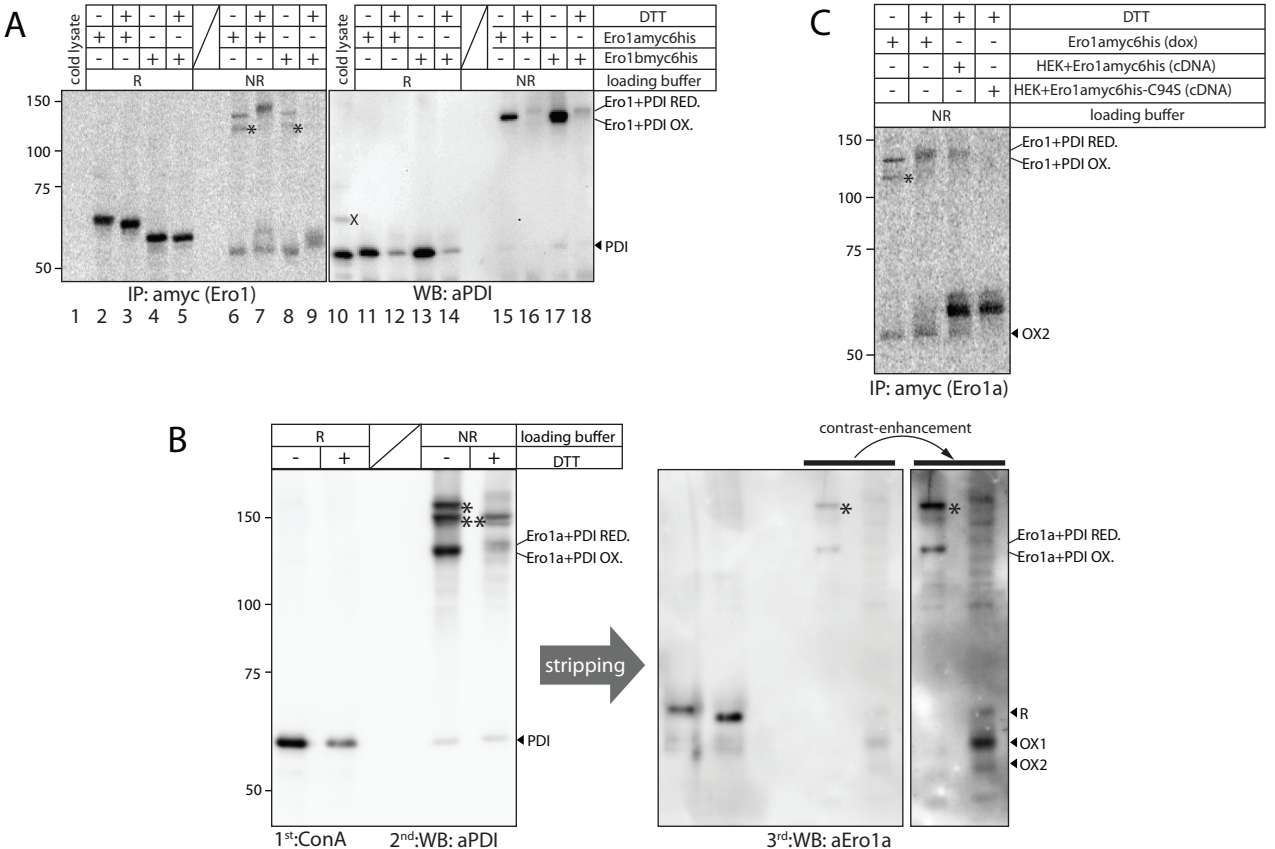

Appenzeller-Herzog et al. Figure 6

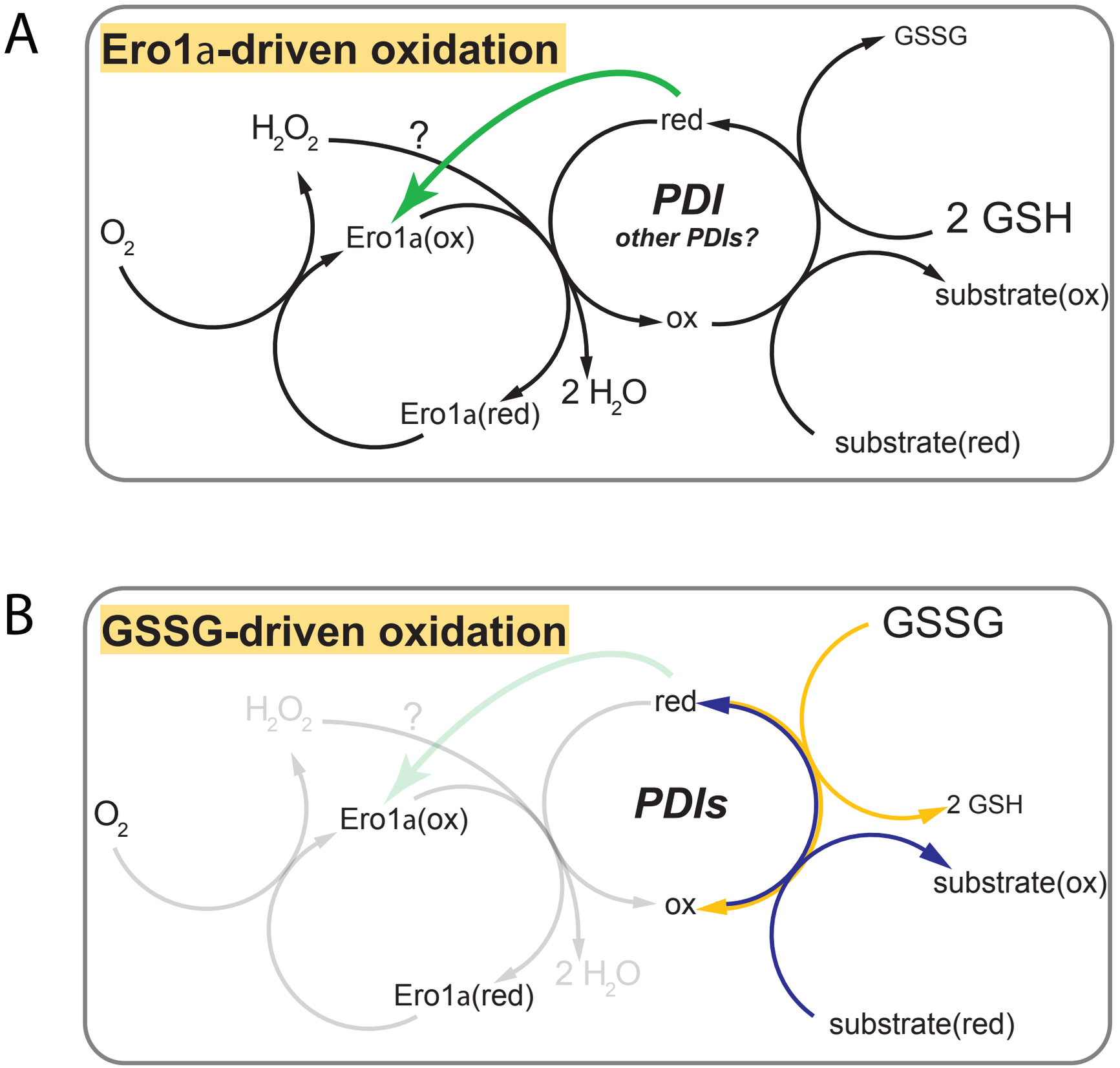

Appenzeller-Herzog et al. Figure 7